national accelerator laboratory

NAL-Pub-74/37-EXP
7200.037

(Submitted to Physical Review)

pp INTERACTIONS AT 300 GeV/c: MEASUREMENT OF THE CHARGED MULTIPLICITY, TOTAL AND ELASTIC CROSS SECTIONS

F. T. Dao, R. Hanft, J. Lach, E. Malamud, and F. Nezrick
Fermi National Accelerator Laboratory, Batavia, Illinois 60510

and

A. Firestone, V. Davidson, D. Lam, F. Nagy, C. Peck, and A. Sheng
California Institute of Technology, Pasadena, California 91109

and

A. Dzierba
Indiana University, Bloomington, Indiana 47401

and

R. Poster, P. Schlein, and W. Slater
University of California, Los Angeles, California 90024

June 1974

NAL-Pub-74/37-EXP
IND-1-74
UCLA-1098

pp Interactions at 300 GeV/c: Measurement of the Charged Multiplicity, Total and Elastic Cross Sections.*

by

A. Firestone, V. Davidson, D. Lam, F. Nagy, C. Peck, and A. Sheng

California Institute of Technology, Pasadena, California, 91109

F. T. Dao, R. Hanft, J. Lach, E. Malamud, and F. Nezrick

National Accelerator Lab., Batavia, Illinois, 60510

A. Dzierba

Indiana University, Bloomington, Indiana, 47401

R. Poster, P. Schlein, and W. Slater

UCLA, Los Angeles, California, 90024

ABSTRACT

In a 35000 picture exposure of the 30-inch hydrogen bubble chamber to a 300 GeV/c proton beam at the National Accelerator Laboratory, 10054 interactions have been observed. The measured total cross section is 40.68 ± 0.55 mb, the elastic cross section is 7.89 ± 0.52 mb, and the average charged particle multiplicity for inelastic events is 8.50 ± 0.12.

*Work supported in part by the U.S. Atomic Energy Commission.

We present data on a determination of the charged particle multiplicity distribution and of the total and elastic cross sections for 300 GeV/c proton-proton interactions. A precise determination of these cross sections and of the shape of the multiplicity distribution are of importance to high energy strong interaction dynamics. The data presented here represent approximately 5.4 times the statistics previously reported at this energy[1].

The primary proton beam was extracted from the National Accelerator Laboratory proton synchrotron and reduced to a suitable intensity for the 30-inch hydrogen bubble chamber. The intensity of the beam was suitably attenuated by closing collimators and defocussing magnets, and by the insertion of an aluminum target approximately 1 km upstream of the bubble chamber. The target was viewed at an angle of 1.5 mrad. Measurements indicated that the beam momentum spread was less than 0.5%. The proton beam entered the bubble chamber with an angular spread of 1.3 mrad. and within this angular region the fraction of contaminating particles is $<0.2\%$[2].

The bubble chamber operated with the following parameters: B = 27kg, 35 mm film, four views, bubble size on film $\sim$15μm, and a bubble density for minimum-ionizing particles of 10-12 bubbles/cm. The entrance window was $\sim$18 cm high by $\sim$5.5 cm wide.

In the first scan the chamber was imaged at 75% of its true size, and all the film was scanned by teams of two physicists working together. In this scan a decision was made as to whether a picture was acceptable based on two criteria: (1) All beam tracks entering the chamber had to be parallel to the beam to $\lesssim$1.3 mrad. Frames with up to 3 off-angle incident tracks were flagged and were also included in the analysis. (2) The number of beam tracks entering through the window as projected in view 2 had to be $\leq$15.

Most rejected frames showed evidence of a hadron shower upstream of the visible hydrogen. With these criteria, 20619 frames were accepted out of 34750 frames taken. The recorded information included the number of entering beam tracks, all events, any secondary interactions, neutron stars, V°'s, kinks, Dalitz pairs, stopping protons, and $\pi\mu e$ decays. The average number of beam tracks per accepted frame was 6.7.

The second scan was performed by professional scanners independently of the first scan, and a third scan was performed by physicists on about 35% of the film to resolve conflicts. In this third scan, event topologies were carefully examined using a magnification of three times chamber size, and conflicts were usually resolved in favor of the second scan. Scanning was done without fiducial cut and 12356 events were found. A fiducial length cut reduced this to our final sample of 10054 events. From the first two scans, the scanning efficiency for the first scan was computed to be (95.1 ± 0.5)% for two-pronged events and (97.9 ± 0.2)% for all other topologies. The second scan efficiency was almost identical to the first, resulting in an overall scan efficiency of 99.7% for two-pronged events and 99.9% for all other topologies. The fiducial length of 53.09 ± 0.14 cm was chosen to allow $\gtrsim$15 cm of visible track length at the downstream end of the chamber in order to minimize the fraction of events of uncertain topology. The quoted uncertainty in the fiducial length includes the effect of uncertainties in the positions of events.

In the determination of the incident proton flux the following sources of systematic error were considered: (i) Beam-track scanning efficiency. This error is neglible as the two independent scans differed by a total of 12 beam tracks out of 138641 incident beam tracks. (ii) Beam contamination. We have no evidence for any beam contamination, but we include a contribution of 0.2% to the error in the overall normalization for possible beam contamination[2].

(iii) Beam attentuation in passing thru the chamber. This results in a systematic reduction in the beam path length of (3.88 ± 0.04)%. The total proton beam path length after all corrections including possible beam contamination is $(7.074 \pm 0.023) \times 10^6$ cm.

To determine the total cross section two additional sources of error were considered: (iv) Contamination in the liquid hydrogen. Measurements indicate the deuterium contamination in the hydrogen is less than 1 part in 10^4, so this error is neglibly small[3]. (v) Hydrogen density. There is an uncertainty of 0.8% in the density of the liquid hydrogen. This comes from a study of the range of 290 muons from π^+ decays at rest in the chamber. We determine the hydrogen density to be 0.0625 ± 0.0005 gm/cm^3.

Elastic events, which constitute about 3/4 of the two-prong sample, were identified by kinematic fitting. All two prong events were completely measured on image plane digitizers at NAL and processed by the standard reconstruction and fitting programs TVGP and SQUAW. From a study of transverse momentum balance, we have concluded that a 3-constraint fit to the elastic hypothesis (with the fast outgoing proton momentum determined by the fit) correctly identifies 92% of all true elastic events. There is a 5% contamination from inelastic events[4]. Corrections for these effects have been included in the quoted cross sections.

The elastic differential cross section is shown in Fig. 1. We have fit the distribution to the function $\frac{d\sigma}{dt} = Ae^{bt}$ in the range $0.04 \leq |t| \leq 0.6$ (GeV/c)^2, and obtain the values $A = 83.82 \pm 2.06$ mb/(GeV/c)^2 and $b = 10.6 \pm 0.3$ (GeV/c)$^{-2}$, with a χ^2 of 7.2 for 9 degrees of freedom. After applying a correction of (17.8 ± 1.2)% to the two-prong sample to account for systematic scanning losses at low t for both elastic and inelastic events[5], we find total and elastic cross sections of 40.68 ± 0.55 mb and 7.89 ± 0.52 mb respectively.

We point out, from Fig. 1, that the elastic differential cross section, extrapolated to t = 0 with constant slope, b, is in agreement with the optical point calculated from our measured total cross section. We have also fit the differential elastic cross section data to a function of the form: $\frac{d\sigma}{dt} = Ae^{bt+ct^2}$ and obtain no evidence of c different from zero[6]. It is worth noting that our measured total cross section is in agreement with the value 40.40 ± 0.28 mb for the total pp cross section, found in a counter experiment at this energy[7]. Our elastic slope may be compared with previous results at this energy[8].

Table I shows the topological cross sections. The raw charged-particle multiplicity data obtained in the scan are found in the column marked "Events Found". In order to obtain an unbiased multiplicity distribution, these data were corrected for the following effects:

(I) Odd prong events. There are a total of 80 odd-prong events. These may be due to an undetectable low-t proton or to an unresolvable secondary interaction close to the primary vertex. The latter effect appears mostly for high multiplicity events, and will be discussed in the next section. The procedure adopted here is to assign all odd prong events to the next higher number of even prongs, and then to correct this revised multiplicity distribution for the effect of close-in secondary interactions.

(II) Close-in secondaries and close-in vees. There are 2947 secondary interactions and 2059 V° decays from events in the fiducial volume. From a study of the distance of secondary interactions and of V°'s from the primary vertex we observe that within 2.2 cm of the primary vertex there is a loss of 46 close-in secondaries and 93 close-in V°'s.

Both of these corrections will lower the multiplicity. The 2947 observed secondary interactions have a distribution heavily peaked at low multiplicity, i.e. 62% 2-prong secondaries, 20% 4-prongs, 9% 6-prongs, 5% 8-prongs, and 4% ≥ 10-prongs. Thus the bulk of this correction lowers the primary multiplicity by only two. Nevertheless, this correction is applied separately for each primary multiplicity according to its observed secondary multiplicity distribution. The close-in V° correction always lowers the primary multiplicity by two.

(III) Dalitz pairs. We calculate that 10054 events should contain 404 Dalitz pairs. The observed number of Dalitz pairs is only 137, and the data have been corrected for the missing Dalitz pairs according to the measured average π° multiplicity as a function of charged particle multiplicity as measured in phase I of this experiment[9].

The column labelled "Corrected Number" in Table I lists the charged particle multiplicities corrected for all the above effects. The quoted errors include the statistical error combined with the errors on the corrections. The cross sections quoted in Table I also include errors due to the uncertainties in the density of the liquid hydrogen and in the total path length.

In Table II we list some of the moments of the charged multiplicity distribution for inelastic interactions only.

We thank the staffs of the accelerator, Neutrino Laboratory, 30-inch Bubble Chamber and Film Analysis Facility at the National Accelerator Laboratory, for their diligent help during the course of this experiment. We also thank Kwan-Wu Lai and Ricardo Gomez for helpful discussions.

Footnotes and References

1) F.T. Dao et al., Phys. Rev. Letters 29, 1627 (1972).

2) The muon contamination in the beam has been measured to be $\leq 0.2\%$. For this measurement the beam intensity was increased by a factor of 22 above normal running intensity, and the bubble chamber was run with a muon shield in the beam line. The number of incident tracks were counted and corrections were made for possible muon scattering out of the beam line.

3) Lou Voyvodic, private communication.

4) In the calculation of the transverse momentum imbalance, the fast outgoing proton was assigned a momentum equal to that of the beam, and its azimuth about the lens axis at the vertex was recomputed using this momentum. The resulting resolution in the transverse momentum is ±100 MeV/c. The uncertainty in this proceedure is reflected in the errors assigned to the elastic and two-prong inelastic cross sections.

5) This correction was made by extrapolating $d\sigma/dt$ from $|t| = 0.04$ $(GeV/c)^2$ to $|t| = 0$ with the same slope, b. We have studied the dependence of the small t correction to the two prong cross section as a function of the missing mass recoiling from the slow identified proton and find no evidence for any such dependence. We believe that this correction to the two-prongs for the systematic scanning loss at low-t applies to both elastic and inelastic two-prongs.

6) The form $\frac{d\sigma}{dt} = Ae^{bt+ct^2}$ may be preferable to the form with c = 0 in the region near $|t| \approx 0.1$ $(GeV/c)^2$, because a "break" in the t-distribution has been reported in this region. See U. Amaldi, in Proceedings of the Second International Conference on Elementary Particles, Aix-en-Provence, France, September, 1973. Nevertheless, although our data do not require

such a "break" in the t-distribution, we find that an arbitrary adoption of the two slopes obtained in the ISR Experiment at approximately this energy (11.57 ± 0.03 and 10.42 ± 0.17 $(GeV/c)^{-2}$ from G. Barbiellini et al. Physics Letters 39B, 663 (1972)) will result in an increase in the elastic cross section in this experiment of only 0.11 mb.

7) H.R. Gustafson et al., Phys. Rev. Letters 32, 441 (1974).

8) S. Childress et al., Phys. Rev. Letters 32, 389 (1974).
V. Bartenev et al., Phys. Rev. Letters 31, 1088 (1973).

9) See Table I of F.T. Dao et al., Phys. Rev. Letters 30, 1151 (1973).

Table I: Topological Cross Sections at 300 GeV

Charged Prongs	Events Found		Corrected Number [a]	Cross Section mb [b]
1	2			
2	2174	All	2662 ± 52	10.29 ± 0.27
		Elastic	2042 ± 108	7.89 ± 0.52
		Inelastic	620 ± 105	2.40 ± 0.51
3	10			
4	1297		1313 ± 37	5.08 ± 0.19
5	4			
6	1490		1509 ± 40	5.84 ± 0.20
7	7			
8	1519		1515 ± 40	5.86 ± 0.20
9	12			
10	1280		1315 ± 37	5.09 ± 0.19
11	5			
12	922		950 ± 33	3.67 ± 0.17
13	13			
14	634		656 ± 28	2.54 ± 0.15
15	6			
16	341		293 ± 22	1.13 ± 0.12
17	9			
18	172		171 ± 15	0.66 ± 0.07
19	8			
20	76		67 ± 11	0.26 ± 0.05
21	3			
22	42		47 ± 8	0.18 ± 0.04
23	0			
24	15		11 ± 5	0.043 ± 0.026
25	1			
26	10		9 ± 4	0.035 ± 0.020
27	0			
28	2		1 ± 1	0.004 ± 0.004
Total	10054		10519 ± 103	40.68 ± 0.55 mb

(a) The total error is the statistical error combined with the errors on the corrections.

(b) The cross section errors contain an additional uncertainty contributed by the hydrogen density and total path length errors.

Table II: Moments of the Multiplicity Distribution

	All Prongs	Negatives Only
$\langle n \rangle$	8.50 ± 0.12	3.25 ± 0.05
$\langle n^2 \rangle$	90.22 ± 1.59	15.05 ± 0.30
$\langle n(n-1) \rangle$	81.72 ± 1.47	11.80 ± 0.25
$f_2 = \langle n(n-1) \rangle - \langle n \rangle^2$	9.45 ± 0.51	1.24 ± 0.13
$\langle n \rangle [\langle n^2 \rangle - \langle n \rangle^2]^{-1/2}$	2.01 ± 0.05	1.54 ± 0.02

Figure Captions

Figure 1: Differential cross section for elastic pp scattering at 300 GeV/c. The data points shown have been corrected for the loss of proton recoils along the lens axis. The very forward points with $|t| < 0.04$ GeV/c suffer additional loss of short recoils at all azimuths about the beam. Those points have not been included in any fit. The smooth curve represents our best estimate of the elastic scattering differential cross section, and is a function of the form $\frac{d\sigma}{dt} = Ae^{bt}$ with $A = 83.82 \pm 2.06$ mb/(GeV/c)^2 and $b = 10.6 \pm 0.3$ (GeV/c)$^{-2}$.

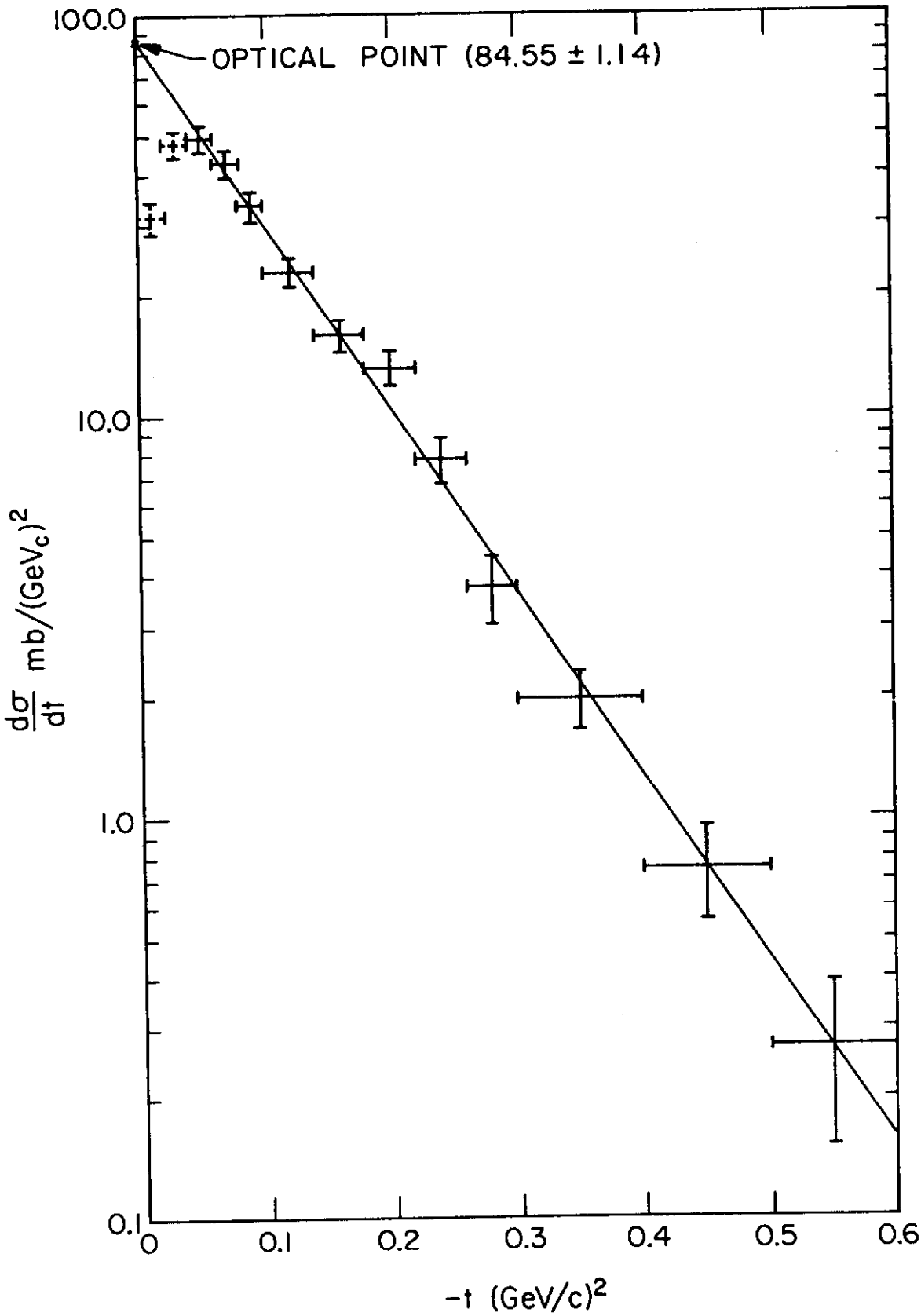
100.0
OPTICAL POINT (84.55 ± 1.14)
10.0
1.0
0.1
0
0.1
0.2
0.3
0.4
0.5
0.6
dσ/dt mb/(GeV/c)²
-t (GeV/c)²

Fig. 1